JOURNAL OF SOLID STATE CHEMSITRY 75, 263–269 (1988)

New Oxyfluorides Containing Indium with Potential Ferroelastic Properties

J. GRANNEC, A. YACOUBI, J. RAVEZ, AND P. HAGENMULLER

Laboratoire de Chimie du Solide du CNRS, Université de Bordeaux I, 351, cours de la Libération, 33405 Talence Cedex, France

Received November 25, 1987; in revised form February 10, 1988

X-ray diffraction, micro-DTA, and microcalorimetric measurements have been performed on compounds of the InF_3–$TiOF_2$, InF_3–MO_2F (M = Nb, Ta), and InF_3–WO_3 systems. Extended domains of solid solutions exhibiting ReO_3-related structures have been detected. Phase transitions of a ferroelastic-prototype nature have been pointed out. In the latter system several domains have been identified, connected with the various allotropic forms of WO_3. The variation of the transition temperatures with composition has been determined. They decrease when indium is substituted to tungsten simultaneously with fluorine to oxygen. © 1988 Academic Press, Inc.

Introduction

Most of trifluorides and oxyfluorides of general formula MX_3 (X = O, F) crystallize at room temperature either with the rhombohedral VF_3 structure ($R\bar{3}c$) or with the cubic ReO_3-type structure ($Pm3m$) when the M^{n+} cation is relatively small ($r_M n+ <$ 0.80 Å) (*1–4*). The structural arrangement can be described in terms of three-dimensional corner-shared octahedra. In some *d*-transition trifluorides, distortions are observed due to the Jahn–Teller configuration of the cations (*5–7*).

A phase transition occurs in the VF_3-type trifluorides; it has recently been announced as being of a ferroelastic-prototype nature, the transition temperature decreasing with increasing cation size (*8, 9*). It seemed, therefore, worthwhile to extend such studies to oxyfluorides and to investigate the influence of formally coupled substitutions, M^{3+}-M^{n+} (M^{n+} being Ti^{4+}, Nb^{5+}, Ta^{5+}, or W^{6+}) and F^-–O^{2-}, on the crystalline symmetry of trifluorides of VF_3-type. InF_3 was selected as starting material according to the large size of the cation (rIn^{3+} = 0.80 Å with CN = 6) (*10*). $TiOF_2$, NbO_2F, and TaO_2F crystallize with the cubic ReO_3 structure. WO_3 presents the following transition sequence:

$$\text{triclinic } (P\bar{1}) \xrightleftharpoons{223\pm5\text{ K}} \text{monoclinic } (P2_1/a \text{ or } P2_1/n) \xrightleftharpoons{590\pm10\text{ K}} \text{orthorhombic (unknown sp. gr.)} \xrightleftharpoons{1000\pm10\text{ K}} \text{tetragonal } (P4/n \text{ or } P4/nmm)$$

(*11–20*). A prototype cubic phase might theoretically be expected at higher temperatures, but evidence has never been found for its formation. Addition of indium trifluoride to WO_3 could also lead to a significant influence on the various transition temperatures of the oxide.

0022-4596/88 $3.00

Preparation

Tungsten trioxide is a commercial product (Aldrich, Gold Label). $TiOF_2$, NbO_2F, and TaO_2F were prepared by reaction of the corresponding oxide with a 40% hydrofluoric acid solution in a platinum crucible, followed by evaporation of the solution to dryness. The obtained oxyfluorides were then heated at 150°C under vacuum and kept in a dry argon atmosphere. InF_3 was obtained by reaction of NH_4HF_2 with In_2O_3, followed by purification under an HF stream at 700°C in order to avoid formation of the InOF oxyfluoride.

The resulting phases were synthesized by solid state reactions from mixtures of InF_3 and the starting oxyfluorides or WO_3 in suitable proportions, in sealed platinum tubes, after preheating under vacuum at 100°C. Due to the different thermal stabilities of the starting materials, the four systems were not investigated at the same temperature. We selected 550°C for the InF_3–$TiOF_2$ system, 700°C for InF_3–MO_2F (M = Nb, Ta), and 800°C for InF_3–WO_3. For the former systems the reactions might be carried out using successive heating cycles at chosen temperatures to prevent thermal degradation. Several annealings were required to obtain pure compounds. All treatments were followed by quenching from reaction temperature to room temperature.

Crystal Chemical Analysis at Room Temperature

X-ray diffraction analysis was performed at room temperature (Philips PW 1710 diffractometer). Some of the solid solutions isolated in the systems studied exhibit a rhombohedral symmetry similar to that of InF_3. For these phases the unit cell taken into account was the rhombohedral pseudo-cubic cell with an α-angle close to 90°C (*21*).

1. The InF_3–$TiOF_2$ System

A solid solution of VF_3-type formulated $In_{1-x}Ti_xO_xF_{3-x}$ was isolated for $0 \leq x \leq 0.50$. For $TiOF_2$ rates higher than 0.50, the decomposition of the oxyfluoride becomes significant and the system can no longer be investigated. The thermal analysis of $TiOF_2$ shows actually that it completely decomposes at 600°C, leading to TiF_4 and TiO_2.

In the studied region, the a-parameter varies from 3.937 to 3.871 Å whereas α increases from 86.81° to 88.18°. The rhombohedral angle, therefore, tends toward 90° in so far as the composition becomes close to that of the cubic phase.

2. The InF_3–MO_2F Systems (M = Nb, Ta)

In the niobium system two regions of solid solutions both formulated as $In_{1-x}Nb_xO_{2x}F_{3-2x}$ have been detected:

—for $0 \leq x \leq 0.68$ the X-ray spectra of the various compositions can be indexed with a rhombohedral symmetry and a unit cell similar to that of InF_3,

—for $0.68 \leq x \leq 1$ the solid solution crystallizes with the cubic ReO_3-type symmetry ($Pm3m$).

No intermediate two-phase region has been detected.

The gradual change of the rhombohedral pseudo-cubic cell (VF_3-type) toward the cubic one is illustrated by the variation of the unit-cell parameters vs composition at 300 K in Fig. 1.

In the InF_3–TaO_2F system no solid solution could be isolated at 700°C.

3. The InF_3–WO_3 System

The X-ray investigation has shown the existence of several homogeneity ranges (Fig. 2):

—in a large composition range ($0 \leq x \leq 0.48$) a rhombohedral solid solution $In_{1-x}W_xO_{3x}F_{3-3x}$ with the VF_3-type structure has been identified,

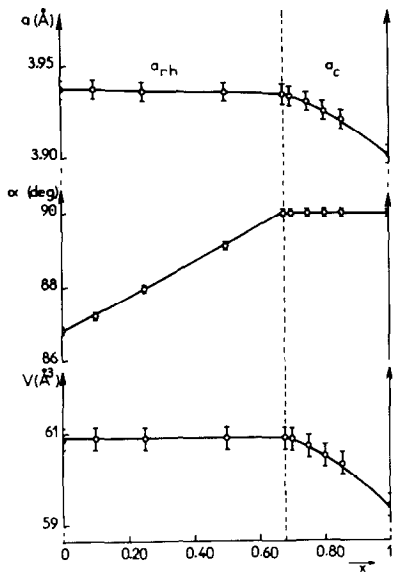

FIG. 1. Change of the unit cell parameters and volume with composition at 300 K for the $In_{1-x}Nb_xO_{2x}F_{3-2x}$ solid solutions.

—a two-phase region appears for $0.48 \leq x \leq 0.89$, in which the border line composition $In_{0.52}W_{0.48}O_{1.44}F_{1.56}$ coexists with a tetragonal phase corresponding to the $In_{0.11}W_{0.89}O_{2.67}F_{0.33}$ composition,

—for $0.89 \leq x \leq 0.96$ a tetragonal ReO_3-derived solid solution has been obtained. The relationships between the tetragonal (t) and the cubic (c) cells are

$$a_t \simeq a_c\sqrt{2} \quad \text{and} \quad c_t \simeq a_c,$$

—in a restricted region ($0.96 < x \leq 0.975$) the powder diffraction patterns show an orthorhombic cell (o) closely related to the previous tetragonal one,

$$a_o \simeq b_o \simeq 2a_c \quad \text{and} \quad c_o \simeq a_c,$$

—for the composition close to WO_3 ($0.975 < x \leq 1$), the structure is closely related to that of monoclinic WO_3 (m).

The variation with composition of the unit cell parameters and volume of the various solid solutions are given in Fig. 2.

Ferroelastic Properties of the Rhombohedral Phases at Room Temperature

By analogy to InF_3 and the homologous trifluorides (*8*, *9*) all rhombohedral solid solutions were expected to have ferroelastic properties at room temperature. These properties result from a strain along the four three-fold axes of the cubic prototype phase. The strain is due to an ω rotation of the fluorine atoms around the three-fold axis and a simultaneous displacement of the cation along this axis (*21–23*).

The variation with composition of the spontaneous strain $e_s = \cos \alpha$ at 300 K is given for the three solid solutions in Fig. 3. The decrease of e_s appears consistent with the fact that the substitution seems to hinder the rotation of the octahedra: the crystallographic determinations show that ω weakens progressively, this effect being particularly significant for the niobium solid

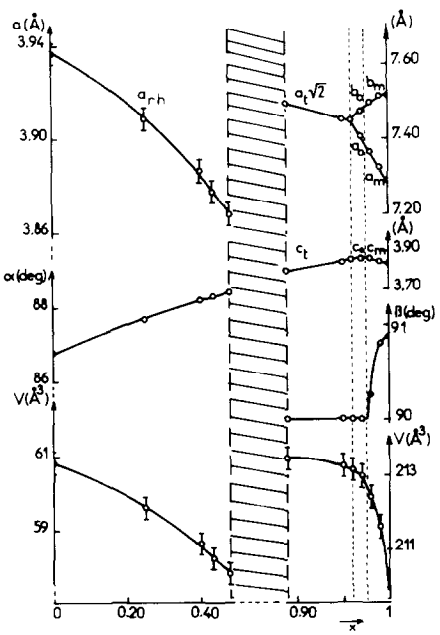

FIG. 2. Change of the unit cell parameters and volume with composition at 300 K for the $In_{1-x}W_xO_{3x}F_{3-3x}$ solid solutions.

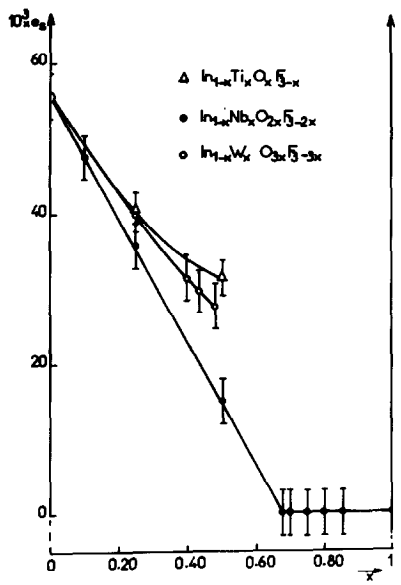

FIG. 3. Variation of the spontaneous strain e_s with composition at 300 K for the $In_{1-x}M_xX_3$ solid solutions exhibiting rhombohedral or cubic symmetry.

solution. The distortion would vanish with increasing oxygen rate and as a consequence lead to the cancelling of e_s.

Phase Transition Investigation

1. Rhombohedral or Cubic Solid Solutions with High InF_3 Concentrations

A microcalorimetric study (home-made apparatus) at low and high temperature has been performed on various samples of the three solid solutions exhibiting rhombohedral or cubic symmetry. The samples were introduced into platinum sealed tubes. A reversible transition was detected for each solid solution, both by heating and cooling.

In order to characterize the symmetry of the obtained allotropic forms, the thermal evolution of the X-ray spectrum was followed using a Guinier–Simon camera, from 77 to 300 K or from 300 to 800 K (Enraf Nonius FR 553), depending on the phase symmetry. As significant examples, Figs. 4–6 show the thermal dependence of the rhombohedral pseudo-cubic unit cell parameters and volume for the compositions $In_{0.50}Ti_{0.50}O_{0.50}F_{2.50}$, $In_{0.50}Nb_{0.50}OF_2$, and $In_{0.52}W_{0.48}O_{1.44}F_{1.56}$, the latter being the upper limit of the corresponding rhombohedral domain. The values of a, α, and V in-

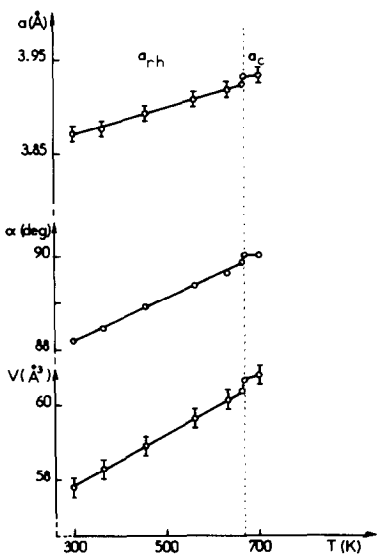

FIG. 4. Thermal dependence of the unit cell parameters and volume for $In_{0.5}Ti_{0.5}O_{0.5}F_{2.5}$.

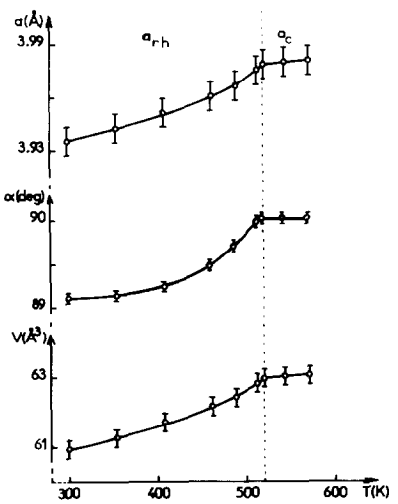

FIG. 5. Thermal dependence of the unit cell parameters and volume for $In_{0.5}Nb_{0.5}OF_2$.

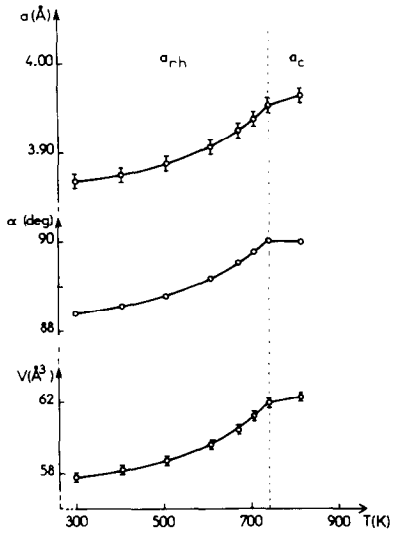

FIG. 6. Thermal dependence of the unit cell parameters and volume for $In_{0.52}W_{0.48}O_{1.44}F_{1.56}$.

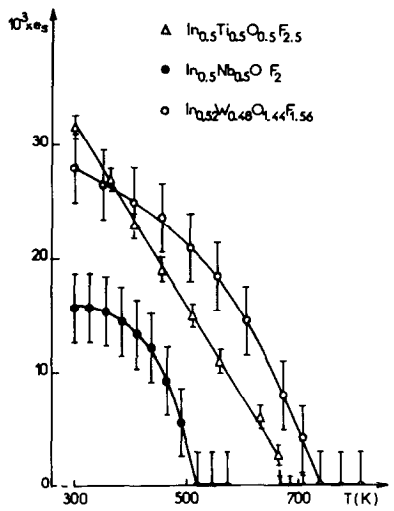

FIG. 7. Thermal dependence of the spontaneous strain e_s for a definite composition of the $In_{1-x}M_xX_3$ solid solutions.

crease up to the transition temperature. Above this temperature, the symmetry becomes cubic: all diffraction lines can now be indexed in the ReO_3-type.

This crystalline system change (rhomb. $R\bar{3}c \rightarrow$ cub. $Pm3m$) implies that the transition is of a ferroelastic-prototype nature (*24*) as previously expected. For each sample the thermal dependence of the spontaneous strain $e_s = \cos \alpha$ is consistent with this assumption, as shown in Fig. 7: e_s decreases regularly and becomes equal to zero at the ferroelastic transition temperature T_t.

In the InF_3–NbO_2F system, i.e., in the only one in which a continuous solid solution $In_{1-x}Nb_xO_{2x}F_{3-2x}$ has been isolated, the symmetry becomes cubic at room temperature for $x \geq 0.68$. For those high x values a cubic–rhombohedral transition has been detected below 20°C, the corresponding transition temperature decreasing with substitution rate. This result is quite consistent with the fact that NbO_2F keeps its cubic symmetry down to 4.2 K.

Figure 8 gives the variation of T_t with composition for the three investigated solid solutions in the rhombohedral and cubic domains. A comparison with Fig. 3 shows that e_s and T_t do not vary similarly: such a

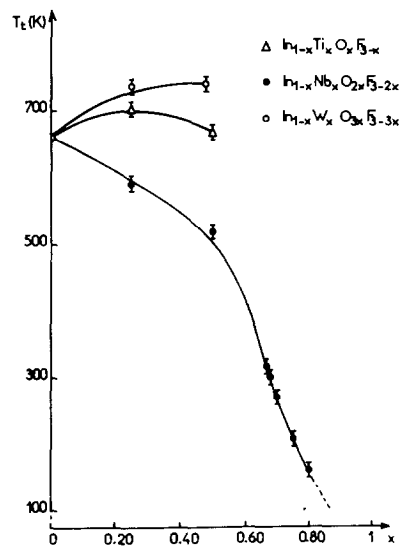

FIG. 8. Variation of the ferroelastic transition temperature with composition for $In_{1-x}M_xX_3$ solid solutions exhibiting rhombohedral or cubic symmetry.

behavior is probably due to the fact that the coupled substitution In^{3+}–M^{n+} and F^-–O^{2-} has to be taken into account and that the symmetries of the starting materials are different. Two competitive effects can be considered to account for the different results obtained for the three solid solutions:

(i) at first the gradual change toward cubic symmetry must lower the transition temperature as the thermal energy necessary to induce the symmetry change decreases,

(ii) on the other hand the substitution of In^{3+} by smaller cations, which could therefore move more easily from their ideal position in the octahedra, should result in increasing values of T_t. Increasing oxygen rate should enhance this tendency.

For $In_{1-x}Nb_xO_{2x}F_{3-2x}$ the first effect is prevailing as the α angle attains rapidly 90°: T_t decreases first progressively, then falls down roughly to become equal to 300 K when $x = 0.68$.

In $In_{1-x}W_xO_{3x}F_{3-3x}$ the small size of W^{6+} leads to larger shifts of anions and cations. T_t consequently increases and then levels off (Fig. 8), as the unit cell becomes simultaneously more symmetrical.

The case of $In_{1-x}Ti_xO_xF_{3-x}$ is intermediate: the Ti^{4+} cation, slightly bigger than W^{6+}, should move less easily. But the variation of α has a predominant influence, since after having reached a maximum the transition temperature decreases again. Moreover, T_t would probably drop further if the solid solution could exist with a wider composition range.

2. *Solid Solutions with High WO_3 Concentrations*

A slight substitution of indium for tungsten and of fluorine for oxygen in WO_3 leads to progressive stabilization at room temperature of the high temperature forms of WO_3.

A micro-DTA study (home-made apparatus (25)) for the composition $In_{0.01}W_{0.99}O_{2.97}F_{0.03}$, which exhibits the monoclinic symmetry at room temperature, allowed us to detect two reversible transitions, at $T_2 = 544 \pm 10$ K and $T_3 = 844 \pm 10$ K, respectively. No other peak has been observed down to 77 K. The thermal variation of the X-ray spectrum was then followed using a Guinier–Simon camera. The diffraction patterns showed the occurrence of transitions from monoclinic to orthorhombic and then to tetragonal symmetry:

$$\text{monocl.} \underset{544\text{ K}}{\overset{T_2}{\rightleftharpoons}} \text{orth.} \underset{844\text{ K}}{\overset{T_3}{\rightleftharpoons}} \text{tetr.}$$

Figure 9 shows the thermal dependence of the unit cell parameters of $In_{0.01}W_{0.99}O_{2.97}F_{0.03}$ from 300 to 940 K. The relationships between the monoclinic (m), the orthorhombic (o), and the tetragonal (t) cells are

$$a_m \simeq b_m \simeq a_o \simeq b_o \simeq a_t\sqrt{2}$$

$$c_m \simeq c_o \simeq c_t.$$

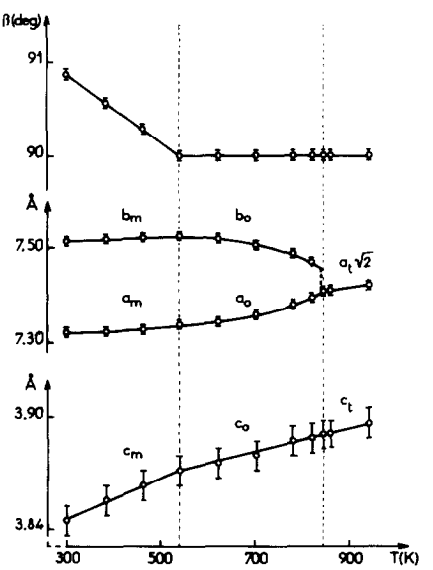

FIG. 9. Thermal dependence of the unit cell parameters for $In_{0.01}W_{0.99}O_{2.97}F_{0.03}$.

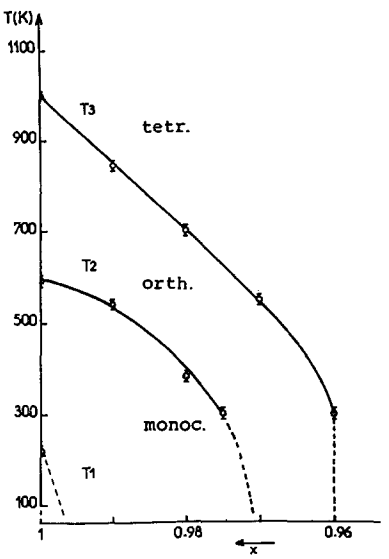

FIG. 10. Variation of the transition temperatures with composition for solid solutions with high tungsten content.

Micro-DTA and X-ray diffraction investigations of the orthorhombic room temperature phases ($0.96 < x \leq 0.975$) only give evidence of an orthorhombic $\rightleftarrows$ tetragonal transition (it occurs at $T_3 = 550 \pm 10$ K for $In_{0.03}W_{0.97}O_{2.91}F_{0.09}$). Powder diffraction patterns obtained at low temperature show that all compounds belonging to this region keep the orthorhombic symmetry down to 77 K.

For the tetragonal room temperature solid solution ($0.89 \leq x \leq 0.96$), this symmetry is maintained over the complete temperature range investigated (77–1073 K).

Figure 10 gives the variation of the transition temperatures for compositions with high tungsten contents. A very weak fluorine–oxygen substitution rate leads to a strong decrease of the WO_3 transition temperatures. In particular, the tricl. $\rightleftarrows$ monocl. transition observed at 223 K for WO_3 has not been detected down to 77 K even for $In_{0.01}W_{0.99}O_{2.97}F_{0.03}$, a composition very close to WO_3.

References

1. K. VORRES AND J. DONAHUE, *Acta Crystallogr.* **8,** 25 (1955).
2. L. K. FREVEL AND H. W. RINN, *Acta Crystallogr.* **9,** 626 (1956).
3. D. BABEL, *in* "Structure and Bonding," Vol. 3, p. 37, Springer-Verlag, Berlin, 1967.
4. D. BABEL AND A. TRESSAUD, *in* "Inorganic Solid Fluorides" (P. Hagenmuller, Ed.), p. 77, Academic Press, New York, 1985.
5. M. A. HEPWORTH AND K. H. JACK, *Acta Crystallogr.* **10,** 345 (1957).
6. F. W. B. EINSTEIN, P. R. RAO, J. TROTTER, AND N. BARTLETT, *J. Chem. Soc. (A),* 478 (1967).
7. R. BOUGON AND M. LANCE, *C. R. Acad. Sci.* **297,** 117 (1983).
8. J. RAVEZ, A. MOGUS-MILANKOVIC, J. P. CHAMINADE, AND P. HAGENMULLER, *Mat. Res. Bull.* **19,** 1311 (1984).
9. A. MOGUS-MILANKOVIC, J. RAVEZ, J. P. CHAMINADE, AND P. HAGENMULLER, *Mat. Res. Bull.* **20,** 9 (1985).
10. R. D. SHANNON, *Acta Crystallogr. A* **32,** 751 (1976).
11. H. BRÄKKEN, *Z. Kristallogr.* **78,** 484 (1931).
12. A. MAGNELI, *Acta Chem. Scand.* **3,** 88 (1949).
13. J. WYART AND M. FOEX, *C. R. Acad. Sci.* **232,** 2459 (1951).
14. R. UEDA AND T. ICHINOKAWA, *Phys. Rev.* **82,** 563 (1951).
15. W. L. KEHL, R. G. HAY, AND D. WAHL, *J. Appl. Phys.* **23,** 212 (1952).
16. G. ANDERSSON, *Acta Chem. Scand.* **7,** 154 (1953).
17. C. ROSEN, E. BANKS, AND B. POST, *Acta Crystallogr.* **9,** 475 (1956).
18. J. A. PERRI, E. BANKS, AND B. POST, *J. Appl. Phys.* **28,** 1272 (1957).
19. S. TANISAKI, *J. Phys. Soc. Japan* **15,** 566 (1960); **15,** 573 (1960).
20. B. O. LOOPSTRA AND P. BOLDRINI, *Acta Crystallogr.* **21,** 158 (1966).
21. J. M. MOREAU, C. MICHEL, R. GERSON, AND W. J. JAMES, *Acta Crystallogr. B* **26,** 1425 (1970).
22. H. D. MEGAW, *Acta Crystallogr. A* **24,** 589 (1968).
23. C. MICHEL, J. M. MOREAU, AND W. J. JAMES, *Acta Crystallogr. B* **27,** 501 (1971).
24. K. AIZU, *J. Phys. Soc. Japan* **27,** 387 (1969).
25. S. MATAR, J. M. REAU, L. RABARDEL, G. DEMAZEAU, AND P. HAGENMULLER, *Solid State Ionics* **11,** 77 (1983).